Signal-to-Noise Analysis for Digital Photography

Rodney Shaw
Hewlett-Packard Research Laboratories, Palo Alto, CA

Abstract

By development of a simple signal-to-noise based model for the DQE of a CCD imaging array plus thermal ink-jet printing, the overall imaging characteristics are expressed in a manner which enables absolute comparisons to be made with any other photographic system, analog or digital. Further, it is demonstrated that in this way other relevant input/output imaging parameters can be evaluated and compared, including the characteristic curve and dynamic range, image noise and overall image quality. In this way the advantages and disadvantages of such a digital photographic system can be expressed in terms of the limiting system parameters by the use of simple mechanistic models.

Introduction

CCD imaging arrays are finding increasing application as image-acquisition components in a variety of digital-imaging contexts, including consumer photography. With the trend towards the availability of larger, high-resolution arrays (and declining cost of manufacture), it might be anticipated that future extension and expansion of these imaging applications will continue at a brisk pace. At the same time both the image quality (and cost) associated with office ink-jet printers has increased dramatically in recent years, to the extent that comparison with the quality of traditional photographic printing has become a question of practical relevance. Thus the combination of these image acquisition and printing technologies offers the opportunity of a digital system capable of overall photographic performance.

The problem of quantifying system performance is ideally suited to an end-to-end signal-to-noise ratio analysis, and it is the purpose of this present investigation to demonstrate the use of a communication-theory based DQE model which includes the most important features of the complete imaging chain. In addition, it is demonstrated that in this way other relevant input/output imaging parameters can be evaluated and compared, including the characteristic curve and dynamic range, image noise and overall image quality. This enables these essential photographic properties to be related back to the CCD and ink-jet parameters, illustrating the roles played, for example, by the multilevel CCD detection and the printer dpi and gray-level capabilities.

DQE Analysis for CCD Imaging Arrays

A simple model for the DQE of a CCD imaging array has recently been published elsewhere[1] along with a comparison between CCD arrays and film.[2] Here only a summary is given.

We assume that digital read-out takes place at m electron levels, denoted by L_1, L_m, according to some specified spacing criterion, perhaps, but not necessarily, linear. In keeping with previous DQE analyses[3] for sequential levels (read-out of every electron) , but where the read-out is now at discrete intervals, we define three statistical functions each involving the weighted average of m Poisson terms, t, and partial sums, S, according to:

$$F_a(q) = (1/m)[S(L_1) + S(L_2) + S(L_3) + ... + S(L_m)] \qquad (1)$$
$$F_b(q) = (1/m)[t(L_1) + t(L_2) + t(L_3) + ... + t(L_m)] \qquad (2)$$
$$F_c(q) = 1/m2)[S(L_1) + 3S(L_2) + 5S(L_3) + ... + (2m-1)S(L_m)] \qquad (3)$$

where, if the basic Poisson term is denoted by $\exp(-q) \, q^r / r!$, the Poisson term $t(L)$ signifies this term for the case $r = L - 1$, while the sum $S(L)$ signifies the sum of all terms from $r = 0$ to $r = L - 1$.

In terms of these statistical functions it is straightforward to show[3] that

$$DQE(q) = qF_b^2(q)/[(1 - F_8(q)) - (1 - F_a(q))^2] \qquad (4)$$

Since $NEQ(q) = q \, DQE(q)$, the noise-equivalent number of recorded quanta can be also be calculated via equation (4). Recall that DQE is a dimensionless efficiency and is usually scaled to 100 %, while NEQ has associated units of (equivalent) number of recorded quanta, and in this case will refer to the number per CCD pixel.

Equation (4) can be thought of generic, in that it reduces naturally to that for mono-sized single-level film grains (of constant quantum efficiency), since in this case the terms and sums in equations (1) to (3) reduce to an appropriate single component. It also reduces naturally to the ideal (sequential-counting) photon detector, when the levels in equations (1) to (3) become sequential. In noting that for film grains the equations reduce to the impractical case of constant quantum sensitivity, whereas in reality photographic grains have a wide spread of quantum efficiencies,

this observation in fact provides the clue for modifying the equations to cope, in the CCD case, with the practical question of count error—i.e., errors induced by detector and counting 'defects' rather than the naturally occurring Poisson 'shot-noise'. For example, whereas an image grain in film may be produced on average by, say, 20 quanta, due to the spread of quantum efficiencies there is no way of telling, after image formation, whether the grain actually received any specific number of quanta between the sensitivity limits, say 4 to 100. Such a spread can be thought of as a serious source of equivalent count-error in the photographic case—in fact this error is one of the main bases of the available dynamic range of photographic recording. In the CCD case dynamic range is provided naturally by the multi-level response—a significant potential DQE advantage.

Based on the above logic, equation (4) remains as definitive, but where equations (1) to (3) are now interpreted in the grain-sensitivity-distribution sense.[3] The terms t(L) and S(L) which in the count-error-free case refer to the (exact) electron level L are now replaced by a summation (with a normalized distribution function) which allows for the fact that due to count-error the level L might in fact have arisen from any one of a spread of actual counts around this level. In other words the count-error is introduced as a distribution function, with this function matching the practical error spread. With this interpretation equation (4) is now more exactly generic, applying to photographic grain, ideal (sequential) photon counters, and CCD counts at discrete electron intervals. It should be noted that in film it is necessary to include another distribution function relating to the influence of the spread in grain sizes, but this is unnecessary here under the assumption that all pixels are the same size.

A final practicality concerns the treatment of the primary quantum efficiency. This is a minor factor in film, since only a small percentage of exposure quanta fail to be absorbed by grains, and thus the majority of quantum efficiency defects are included within the sensitivity-distribution analysis, as discussed above. However for CCDs this may be the most serious inefficiency in the entire imaging process. Inclusion of the primary quantum efficiency in the DQE model is a trivial step, if we first consider the statistics of the conversion process from exposure quanta to CCD electrons. The selection from the exposure quanta, q, can be considered to be a binomial process of mean value, η, and since a Poisson distribution with a binomial filter yields a preserved Poisson, the resulting number of electrons $e = \eta q$ will hence also be Poisson. However, rather than replace q by ηq everywhere in equations (1) to (4), it is simpler merely to consider the binomial filter as an equivalent exposure shift, which in DQE terms may be expressed by

$$DQE(\eta q) = \eta \, DQE(q) \qquad (5)$$

With appropriate substitution in equation (4), i.e., with the primary quantum efficiency as a linear multiplier, this important parameter is now included in the analysis.

Imaging Characteristics of Ink-Jet Printing

We first consider a simple model for the image noise associated with binary ink-jet printing, as recently published elsewhere.[4] This may be expressed on a digital noise scale (DNS) as

$$DNS_{binary} = (25,400/dpi) \, SqRt[(rw - R)(R - rb)] \qquad (6)$$

where the digital noise scale is defined in terms of the square root of the low spatial frequency value of the *pixel-sampled* noise-power spectrum in *reflectance* units. In this model dpi denotes the pixel pitch in terms of dots-per-inch and R denotes the mean image reflectance, where it is assumed that this mean reflectance is obtained by a binomial mix of "black" elements, with constant reflectance rb, and "white" elements, rw. In this form the model is essentially for the binary printing of grays in the absence of incoming noise. It can readily be extended to multi-level printing by allowing rb to assume a series of values, for example matching the available discrete gray ink reflectances. If m such levels are available, it is easy to show that according to the model the maximum image noise level will be given by

$$DNS_{multilevel}(max) = 12,700 / (m \, dpi) \qquad (7)$$

The advantage of the digital noise scale as expressed is terms of the square-root-reflectance-power-spectrum is it provides an absolute scale which also approximates to perceived noise,[4] and can readily be mapped to exisiting descriptors for analog photographic grain. For example, on this scale a value of 2 corresponds to *very fine grain*, 4 to *medium grain*, and 6 to *coarse grain*, with the full photo-graphic gamut typically falling within the range 1 to 10. These values, along with the model of equation (7), provide a simple recipe for the combinations of printing gray levels and dpi which may be used to achieve photographic quality by use of a digital printer.

When there is incoming noise, as for example in the case of digital photography where such noise will be due to the photons in the original scene as transduced by the CCD imaging array plus A-to-D conversion (with their own appropriate additive and multiplicative noise mechanisms), the total printed noise will be larger than that predicted by equation (7), and it is important in the design of an overall digital system that this increase should be kept to a minimum.

Note that in this context it is implicit from the perception model that the noise will be minimized if the m printer gray levels are spaced in equal reflectance increments. Note also that this number of gray levels (m) has been

denoted in the same terms as the number of digital levels acquired by the CCD imaging array, due to the obvious implication that each captured scene level must be mapped into print space. It is thus implied that mapping the acquired levels at equal reflectance increments in the print will minimize the perceived image noise.

CCD + Ink-Jet Model

With the above models in place for the CCD and ink-jet components, along with the assumption of mapping the m acquired count-levels into m equally spaced printer reflectance-states, we now have an overall model by which we can calculate the end-to-end DQE or any similar system performance characteristic. To do this it is necessary to assume numerical values for the respective CCD and ink-jet parameters. As an illustrative exercise of the capability of the overall model a set of parameters has been chosen to be indicative, rather than representative of any existing practical devices.

We assume that a CCD pixel is 5×5 microns and that the primary quantum efficiency of detection is 0.125, recalling that this is a linear multiplier of DQE. Following this lossy process pixel read-out takes place at 64 count levels, corresponding to 10, 20, 30, 640, electrons, i.e., in effect at 80, 160, 240, 5120 exposure photons. The total count-error is assumed to be assumed uniform with an amplitude of 10 electrons (i.e., the width of an individual count-increment). Mapping of the 64 count-levels to the printer then takes place at 300 dpi in equal increments of reflectance. Note that this implies that a 5 micron CCD pixel is mapped to approximately 85 microns in the print, which could be achieved, for example, by mapping to a 4×4 half-tone array with a printer capable of 4 gray-levels at 1200 dpi.
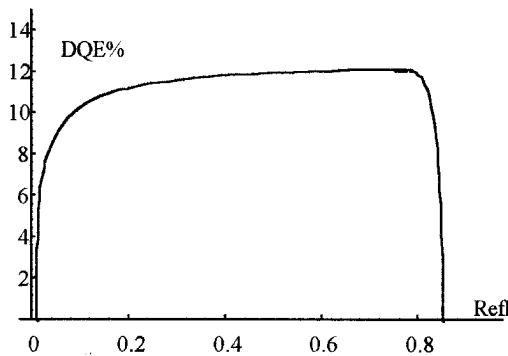

Figure 1. Model DQE characteristics for CCD+TIJ .

First we consider the overall DQE characteristics, shown in Figure 1 as the function of the mean print reflectance. Several features of this curve are of significance, not the least of which is the fact that the introduction of count-spacing and error functions implies only minor subsequent loss in DQE terms (recall that the assumption

made for the primary quantum efficiency itself limits the DQE to 12.5%). Also, we note the constant nature of DQE over the reflectance range, and contrast this behavior with that of an overall conventional photographic neg-pos system which typically has non-linear DQE characteristics peaking at values of around 2% towards higher print reflectance levels.

Although not the focus of this study, the same model allows calculation of the mean-level system input-output characteristics, as shown for example in Figure 2. Here the mean print reflectance is shown as function of the log of the exposure at the CCD array (in absolute terms of photons per square-micron at the CCD).
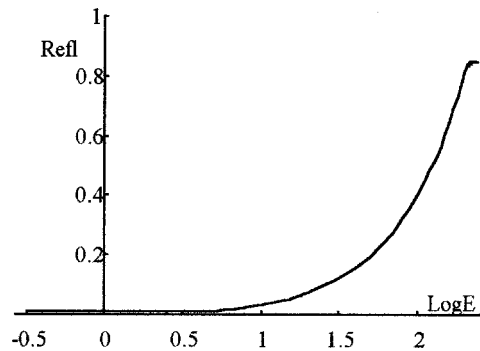

Figure 2. Model mean-level characteristics for CCD+TIJ.

The output image noise characteristics are of more interest in the present context, and these are shown in Fig. 3 in terms of the digital noise scale. The interesting feature of this curve is the implication that the output perceived noise is everywhere within traditional "photographic-space", falling mainly in the *fine* to *very-fine-grain* category.
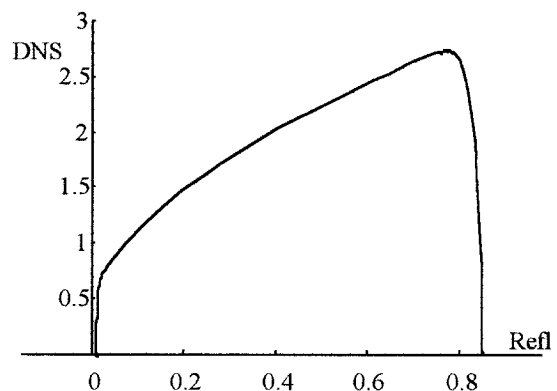

Figure 3. Model image noise characteristics for CCD+TIJ.

Finally we consider the question of overall image quality. Although this question has been answered implicitly by the combined nature of the system DQE and noise characteristics, it can be specifically addressed in terms of the

number of noise-equivalent quanta recorded in the output print. Several studies have been made covering a broad range from low quality to very high quality prints, and these have indicated that either a logarithmic or square-root transformation of the recorded NEQs correlates well with the perception of overall quality (see for example Reference 5). Here a square-root measure is adopted, based on arguments concerning the square-root nature of the signal-to-noise ratio associated with the photon exposure itself.

Figure 4 shows the square-root-NEQ characteristics as calculated according to the same set of system parameters. Also shown, for interest, is the overall quality associated with the original photon exposure—i.e., that which would have resulted from an ideal image acquisition plus printing system. Both curves have been calculated on the basis of the number of NEQs (and hence the signal-to-noise ratio) associated with a single 300 dpi pixel in the printed image.
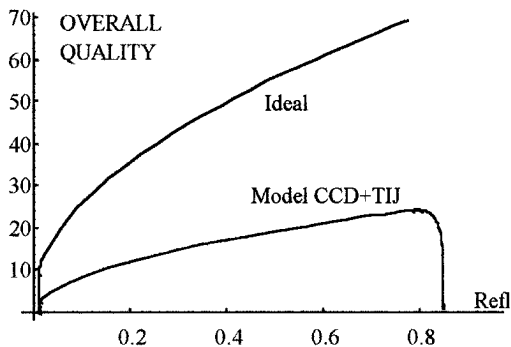

Figure 4. Model signal-to-noise ratio characteristics for CCD+TIJ .

Separate considerations[5] lead to the conclusion that the model Square-root-NEQ values shown in Fig. 4 comfortably exceed those required to produce an acceptable photographic print, but these considerations are beyond the scope of the present study. It should be noted that the plots of both Figures 3 and 4 scale directly with the effective dpi which is used to map a single projected CCD pixel. For example, if a value of 150 dpi had been assumed, the noise levels of Figure 3 would be doubled while the square-root-NEQs of Figure 4 would be halved. This raises the separate question of the effective degree of print "enlargement" from the CCD "negative", a practical consideration which naturally invokes the question of the size of the CCD pixel array, and again, this is beyond the scope of this present model study.

Conclusions

An end-to-end signal-to-noise ratio model has been developed for a digital photography system exemplified by the combination of a CCD imaging array and ink-jet printing. This analysis allows important imaging performance characteristics to be mapped from scene to print—including, noise, DQE and overall quality—as well as the associated characteristic curve (mean-level input/put).

Illustrative examples have been shown to highlight the influence of various fundamental parameters associated with CCD arrays and ink-jet printing, and it has been demonstrated an appropriate combination of these technologies may be capable of producing prints which are comparable with traditional photographic prints.

Further digital optimization optimization studies based on this model approach will be reported in future publications.

References

1. R. Shaw, *SPIE Medical Imaging Symp*, CA, Feb. 1997.
2. R. Shaw, *Ibid*.
3. J. C. Dainty & R. Shaw, *Image Science*, Academic Press, 1974.
4. R. Shaw, *IS&T Proc. : NIP 12*, 162 (1996).
5. J. Holm, *J. Soc. Sci. Technol.* Japan, **59**, 117 (1996).